**ONLINE SUPPLEMENT**

# Protective effects of activated myofibroblasts in the pressure overloaded myocardium are mediated through Smad-dependent activation of a matrix-preserving program

Ilaria Russo[1], Michele Cavalera[1], Shuaibo Huang[1], Ya Su[1], Anis Hanna[1], Bijun Chen[1], Arti V Shinde[1]

Simon J Conway[2], Jonathan Graff[3], and Nikolaos G Frangogiannis[1]*

## Supplemental Methods:

**Generation of mice with myofibroblast-specific loss of Smad3**: In order to study the role of Smad3 in fibroblasts in the pressure-overloaded myocardium, we generated mice with loss of Smad3 in activated myofibroblasts (FS3KO). We used a transgenic mouse line in which Cre recombinase was driven by a 3.9-kb mouse *Postn* promoter [1,2]. Periostin, which is encoded by *Postn*, is not expressed in cardiomyocytes, vascular cells, hematopoietic cells or quiescent cardiac fibroblasts [3, 4], but is upregulated in injury site-fibroblasts in infarcted and in pressure-overloaded hearts [4,5]. Postn-Cre mice were bred with Smad3 fl/fl mice [6,7] to generate Postn-Cre Smad3 fl/fl animals and corresponding Smad3 fl/fl controls.

**Mouse model of cardiac pressure overload induced through transverse aortic constriction (TAC)**: Animal studies were approved by the Institutional Animal Care and Use Committee at Albert Einstein College of Medicine and conform with the Guide for the Care and Use of Laboratory Animals published by the National Institutes of Health. Male and female, 2-6 month-old Smad3 fl/fl (n=30) and FS3KO (n=33) mice in a C57/BL6 background underwent pressure overload protocols. Animals were anesthetized with inhaled isoflurane. Aortic banding was achieved by creating a constriction between the right innominate and left carotid arteries as previously described [8, 9]. The degree of pressure overload was assessed by measuring right-to-left carotid artery flow velocity ratio after constricting the transverse aorta. Experiments with a right to left carotid flow ratio< 3 or >20 were excluded. At the end of the experiment, the heart was excised, fixed in zinc-formalin, and embedded in paraffin for histological studies. Hearts used for histological analysis were sectioned from base to apex at 250μm intervals. Animals underwent 7-28 days of banding. At the end of the experiment, euthanasia was performed using 5% inhaled isoflurane. Early euthanasia was performed with the following criteria, indicating suffering of the animal: weight loss>20%, vocalization, dehiscent wound, hypothermia, clinical signs of heart failure (cyanosis, dyspnea, tachypnea), lack of movement, hunched back, ruffled coat, lack of food or water ingestion.

**MMP-8 inhibition experiments:** In order to study the effect of MMP8 inhibition on the pressure-overloaded myocardium, a cohort of Smad3 fl/fl (n=31) and FS3KO (n=33) mice was randomly assigned to undergo TAC procedure and to receive MMP8 inhibitor (MMP8i, 5mg/kg, i.p., Calbiochem, cat#444237, San Diego, CA) or vehicle control (VEH, 1% DMSO dissolved in 0.9% sterile saline). Animals were injected 30 minutes before instrumentation, were treated daily for 6 days after TAC and euthanized at day 7 after echocardiographic studies.

**Echocardiograph**y: Echocardiographic studies were performed before instrumentation, 7 and 28 days after TAC using the Vevo 2100 system (VisualSonics. Toronto ON), as previously described [10]. Long-axis M-mode and short-axis M-mode were used for measurement of systolic and diastolic ventricular diameter and wall thickness. The left ventricular end-diastolic diameter (LVEDD), left ventricular end-systolic diameter (LVESD), left ventricular end-diastolic volume (LVEDV), and left ventricular end-systolic volume (LVESV) were measured as indicators of dilative remodeling. Left ventricular mass (LV mass) was measured as an indicator of hypertrophic remodeling. Fractional shortening (FS = [LVEDD - LVESD] ×100/LVEDD) and ejection fraction (LVEF = [LVEDV – LVESV] ×100/LVEDV) were calculated for assessment of systolic function.

**Mitral inflow Doppler, tissue Doppler imaging and assessment of diastolic function**: Images from apical 4-chamber view were acquired to assess LV filling and diastolic function. Transmitral LV inflow velocities were measured by pulsed-wave Doppler. Peak early E (E wave) and late A (A wave) filling velocities, E/A ratio, and deceleration time (DT) of early filling velocity were measured. Tissue Doppler Imaging (TDI) was obtained placing a 1.0mm sample volume at the medial annulus of the mitral valve. Analysis was performed for the early (e′) and late (a') diastolic velocity. The mitral inflow E velocity to tissue Doppler e' wave velocity ratio (E/e') and tissue Doppler early e' velocity to tissue Doppler late a' velocity ratio were calculated to assess diastolic function. All Doppler spectra were recorded for 3-5 cardiac cycles at a sweep speed of 100mm/s. The color Doppler preset was at a Nyquist limit of 0.44 m/s. The echocardiographic off-line analysis was performed by an investigator (I.R.) blinded to the study groups.

**Immunohistochemistry and histology**: For histopathological analysis murine hearts were fixed in zinc-formalin (Z-fix; Anatech, Battle Creek, MI), and embedded in paraffin. Sections were cut at 5 μm from base to apex at 250 μm intervals as previously described [10]. In order to label the collagen fibers one section from each partition was stained using picrosirius red. Replacement fibrosis, interstitial fibrosis and perivascular fibrosis were quantitatively assessed using Axio Vision LE (version 4.8, Carl Zeiss, Oberkochen, Germany) or Image-Pro Plus software (version 4.5.0.29, Media Cybernetics, Rockville, MD). Replacement fibrosis was defined as an area of myocardium where cardiomyocytes were replaced by fibrous tissue. Areas of replacement fibrosis were traced at 3 different levels (basal, mid-myocardial, apical) and expressed as a percentage of the total left ventricular area. Interstitial fibrosis was assessed in areas without replacement fibrosis as the percentage of the left ventricular area stained for collagen. For each mouse, 15 different fields of the left ventricle from at least 3 different sections were used for quantitation. Perivascular fibrosis was measured by assessing the area of periadventitial collagen in 6 intramyocardial coronary vessels from each animal. The ratio of periadventitial collagen to the medial area of the vessel was used as an indicator of perivascular fibrosis. Myocytolysis was defined histologically as evidence of sarcomeric loss in cardiomyocytes. The myocytolysis score was assessed for each animal by examining sections stained with hematoxylin and eosin, considering both the number of cells with myocytolysis and the severity of myofibrillar loss in each cell. Eight to twelve different regions of left ventricle and at least 20-30 cardiomyocytes from each section were visualized. Each cell with myocytolysis was scored on the basis of the extent of myofibrillar loss (score 1 <25%, score 2 $\geq$25% and <75%, score 3$\geq$75%). The myocytolysis score for each field was measured by adding the scores for all cardiomyocytes with evidence of myocytolysis. The myocytolysis score for each mouse was calculated as the average of the scores of all fields.

To examine MMP8 localization and to measure the density of MMP8+ interstitial cells, histological sections were stained immunohistochemically with a rabbit anti-mouse MMP8 antibody (dilution 1:100; Abcam, Cambridge, MA). Staining was performed with the use of a peroxidase-based technique with the Vectastain ELITE rabbit kit (Vector Laboratories Inc., Burlingame, CA). Sections were pretreated with a solution of 3% hydrogen peroxide to inhibit endogenous peroxidase activity and incubated with 2% bovine serum albumin (Sigma-Aldrich, St. Louis, MO) to block nonspecific protein binding. Peroxidase activity was detected with diaminobenzidine with nickel. Negative controls were performed with the use of normal rabbit IgG. Tissues from kidney and spleen were used as positive controls for MMP8 immunohistochemistry. Slides were counterstained with hematoxylin. Immunofluorescence staining was performed with the use of the following antibodies: rat anti-mouse Mac-2 antibody (dilution 1:200, Cedarlane Laboratories, Burlington, Ontario, Canada), rabbit anti–inducible nitric oxide synthase (iNOS) antibody (dilution 1:100; Abcam, Cambridge, MA), and rabbit anti-Arginase-1 (Arg1) antibody (dilution 1:100, Cell Signaling Technology, Danvers, MA) Quantitative assessment of the density of MMP8-expressing cells, Mac-2, iNOS and Arg1-positive macrophages was performed by counting the number of cells in at least 5 random fields from 2-3 different sections from each heart with the use of ImageJ software. Cell density was expressed as cells/mm2. Quantitative histology was performed by an investigator (I.R.) blinded to the study groups.

**TUNEL apoptosis assay:** Identification of apoptotic cardiomyocytes and non-cardiomyocytes in pressure-overloaded hearts was performed using the DeadEnd™ Fluorometric TUNEL System (Promega, Cat# G3250) and WGA staining (to visualize cardiomyocytes by labeling cell membranes and the surrounding extracellular matrix) [11]. Apoptotic cardiomyocytes and non-cardiomyocytes were counted in 10 different fields from each mouse.

**Dual immunofluorescence:** For studies examining inflammatory activation of macrophages, dual immunofluorescence combining staining for the macrophage marker Mac2 and iNOS or Arg1 was performed. Quantitative assessment of the density of macrophages-expressing iNOS or Arg1 was done by counting the number of cells that showed dual fluorescence in at least 5 random fields from 2 different sections of each heart using the Axio Vision LE software (version 4.8, Carl Zeiss, Oberkochen, Germany). Density of the iNOS and Arg1 positive macrophages was expressed as cells/mm2.

**Assessment of collagen denaturation using labeling with the Collagen hybridizing peptide**: In order to assess fragmentation of the collagen network, we used labeling with a peptide that specifically binds to unfolded collagen[12,13]. A Collagen Hybridizing Peptide 5-FAM conjugate (F-CHP, 3Helix, Inc., Salt Lake City, UT) was used to detect denatured collagen in pressure-overloaded heart sections using fluorescent labeling. Sections were counterstained with WGA to label the cardiac interstitium. . At least 5 randomly selected fields from 2-3 different sections from each heart were scanned, in order to quantify the ratio of the area stained for CHP (area of collagen fragmentation) to the total left ventricular area of the section using ImageJ software. Quantitative analysis was performed by an investigator (A.H.) blinded to the study groups.

**Mass spectrometry**: In order to assess the serum levels of the pro-inflammatory collagen-derived matrikine *Proline-Glycine-Proline* (PGP) as biomarker of collagen fragmentation, Smad3 fl/fl (n=5) and FS3KO (n=7) mice were euthanized after 7 days of TAC, blood was collected from the inferior vena cava and serum was obtained for mass spectrometry analysis at the Albert Einstein College of Medicine Proteomics Core. The tripeptide PGP was measured by LC-MS/MS (liquid chromatography-tandem mass spectrometry) using a modified method of Rowe, et.al.[14]. The mobile phase for LC separation consisted of 0.1% formic acid (FA) in deionized water (A) and in acetonitrile (B) performed on the Agilent 1290 UPLC system. The flow rate was 0.35 mL/min and 10 µl of sample was injected approximately every 7 min at 1% B for 0.5 min. After 1 min %B was increased to 95% and held for 1 min. Within 1 min %B was decreased to 1% and held for 3 additional minutes for column equilibration. The column consisted of a Zorbax Eclipse Plus C18 RRHD; 1.8 microns; 2.1 X 150 mm (Agilent) operated at 40 °C. The 6490 QqQ (triple quadrupole) mass spectrometer (Agilent) was operated using multiple reaction monitoring (MRM) and optimized for PGP using commercial standards (AnaSpec EGT Group) in water and diluted mouse serum (1:1; v/v). The MRM precursor to product ion transitions for PGP are m/z 270.1 to 70.0 (quantifier) and to 173.0 (qualifier) similar to Rowe, et.al.[14] with collision energies of 15 volts. The first minute after each sample injection was diverted to waste and MS data was collected for the next 2 min. Stock solutions of 5 mg/mL of PGP were diluted down to 50 ng/mL in 1% methanol/water containing 0.1% FA and to 5 ng/mL in diluted mouse serum. Serial dilutions in 1% methanol/0.1% FA water (12 points; 1:1 v/v; 100 µl) and in diluted mouse serum (10 points; 1:1 v/v; 40 µl) was performed and transferred to 96 well plates for determining calibration curves and lower limit of detection (LLOD). A linear least squares fit calibration curve was used and the coefficient of determination was 0.998. The lower limit of detection for PGP was 0.08 ng/mL. The serum samples were diluted 1:1 v/v (40 microliters) and analyzed by LC-MS/MS in triplicate.

**Isolation and culture of cardiac fibroblasts**: Fibroblasts were isolated from WT C57/BL6J or Smad3 KO[11] mouse hearts then cultured in collagen pads, as previously described[15,11]. WT and Smad3 KO cardiac fibroblasts were cultured to passage 2 and serum-starved overnight. Collagen matrix was prepared by diluting a stock solution of rat 3.0 mg/ml collagen I (GIBCO Invitrogen Corporation, Carlsbad, CA) with 2x DMEM and distilled water for a final concentration of 1 mg/ml collagen. Cell suspensions were mixed with collagen solution to achieve the final $3*10^5$ cells/ml concentration. Subsequently, 500 µl of this suspension was aliquoted to a 24-well culture plate (BD Falcon, San Jose, CA) and allowed to polymerize at 37ºC for 30 min. Following polymerization, the pads were released from the wells, transferred to 6-well culture plate (BD Falcon, San Jose, CA) and cultured in 0% FCS DMEM/F12 or in presence of TGF-β1 (10ng/ml), TGF-β2 (10ng/ml), TGF−β3 (10ng/ml), activin A (50ng/ml), activin B (50ng/ml), myostatin (100ng/ml), or GDF-11 (10ng/ml) (all from R&D systems) for 24 h. In order to study the effects of non-Smad pathways on fibroblast gene expression, WT and Smad3 KO cardiac fibroblasts were pre-treated with the Erk inhibitor U0126 (Sigma, 10µM) in the presence or absence of TGF-β1. In order to investigate the role of p38 MAPK, cells were pretreated with SB203580 (Sigma, 20µM).

In order to study the effects of TGF-βs, BMPs, and angiotensin II on Smad3 phosphorylation, cardiac fibroblasts were cultured in plates for 30 min in the presence or absence of TGF-β1 (10ng/ml), TGF-β2 (10ng/ml), TGF−β3 (10ng/ml) (all from R&D Systems), BMP2 (50ng/ml), BMP4 (50ng/ml), BMP7 (50 ng/ml) (from Peprotech), or angiotensin II (50ng/ml, Sigma). Cell lysates were used for protein extraction.

In order to study the effects of TGF-β1 and Smad3 loss on MMP8 expression and release, cardiac fibroblast from WT C57/BL6J or Smad3 KO mouse hearts were cultured in plates for 30 min, 4h or 12h in the presence or absence of TGF-β1 (10ng/ml). The supernatant was used to assess MMP8 protein levels and activity. MMP8 protein levels in the supernatant were measured using a mouse MMP8 ELISA kit (LSBio, LS-F39808). MMP8 activity was measured using a SensoLyte® 520 MMP-8 fluorimetric assay kit (AnaSpec, AS-71154). Recombinant mouse MMP8 (R&D, 2904-MP) was used as positive control.

**Isolation of fibroblasts from pressure-overloaded hearts**: Fibroblasts were isolated from pressure-overloaded hearts after 7 days of TAC for western blotting and RNA extraction as previously described [9]. Gene expression in fibroblasts harvested from pressure overloaded hearts was compared between Smad3 fl/fl and FS3KO mice (n=5/group).

**Isolation and culture of bone marrow-derived macrophages**: Preparation of bone marrow-derived macrophages was performed as previously described by Stanley ER[16]. Briefly, bone marrow macrophages from WT C57/BL6J mice (n=15) were isolated from femurs and tibiae and cultured in the presence of WEHI conditioned media for 3 days. In order to obtain macrophage differentiation, cells were then cultured in plates in the presence of incremental concentrations of CSF-1 (12ng/ml and 120ng/ml) for 5 days and serum-starved overnight (16 hrs). In order to study the effects of MMP8 on macrophages phenotype, cells were treated for 24 hours with murine recombinant MMP8 (1ng/ml or 50ng/ml, R&D Systems, Minneapolis, MN), activated according to the manufacturer protocol. Levels of active TGF-β1 and CCL2 were assessed using commercially available ELISA assays (for CCL2: mouse CCL2/JE/MCP-1 Quantikine ELISA Kit, R&D systems Cat# MJE00B; for active TGF-β1: LEGEND MAX™ Free Active TGF-β1 ELISA Kit with Pre-coated Plates, Biolegend, Cat#437707).

**RNA extraction and qPCR**: Total RNA was extracted from cells and mouse hearts, cDNA was amplified using the SsoFast EvaGreen Supermix reagent and the C1000 thermal cycler apparatus from Bio-Rad following the manufacturer's recommendations. The following primer pairs were used: Smad3 forward 5'-CACAGCCACCATGAATTACG-3', Smad3 reverse 5'-TGGAGGTAGAACTGGCGTCT-3', Mmp2 forward 5'-TTCAACGGTCGGGAATACAG-3', Mmp2 reverse 5'-AACTTGCAGGGCTGTCCATC-3', Mmp3 forward 5'-TCAGTGGATCTTCGCAGTTG-3', Mmp3 reverse 5'-AGGATGCCTTCCTTGGATCT-3', Mmp8 forward 5'-TTTGATGGACCCAATGGAAT-3', Mmp8 reverse 5'-GAGCAGCCACGAGAAATAGG-3', Mmp9 forward 5'-CCGACTCCAGCCCTTTTATT-3', Mmp9 reverse 5'-GAGTGGATAGCTCGGTGGTG-3', Timp1 forward 5-ATTCAAGGCTGTGGGAAATG-3', Timp1 reverse 5'-CTCAGAGTACGCCAGGGAAC-3', Timp2 forward 5'-ACAGACTTCAGCGAATGGA-3', Timp2 reverse 5'-CTTGGGAAGCTTGAGAGTGG-3', Tgf-β1 forward 5'-AATCAAGTGTGGAGCAACATG-3', Tgf-β1 reverse 5'-AGCCCTGTATTCCGTCTCCT-3', Col1 forward 5'-CGAGGTATGCTTGATCTGTA-3', Col1 reverse 5'-ACATCTTCTGAGTTTGGTGATA-3', Fibronectin forward 5'-GAAGACAGGACCAATGAA-3', Fibronectin reverse 5'-ATAGACACTGACTTCGTATT-3', Tenascin-C forward, 5'-ACTATCACAATGGTAGAT-3', Tenascin-C reverse 5'-CGATGACAGTTCTTATAC-3', Tsp1 forward 5'-TCAGACTATGTAGATATGCTATT-3', Tsp1 reverse 5'-AAAGGGTATTGGCAAAGA-3', Tsp2 forward 5'-ATCTACACCTCCTTCATC-3', Tsp2 reverse 5'-GCCTCATATCTCATCCAA-3', Sparc forward 5'-AACTCTCTCCCTCTGATG-3', Sparc reverse 5'-AATCTATGTTAGCACCTTATC-3', Opn forward 5'-AGTAAGGAAGATGATAGGTA-3', Opn reverse 5'-TATCCACTGAACTGAGAA-3', Ccn2 forward 5'-CCGACTGGAAGACACATT-3', Ccn2 reverse 5'-GCAGAAGGTATTGTCATTGG-3', Gapdh forward 5'-CGACTTCAACAGCAACTC-3', Gapdh reverse 5'-GTAGCCGTATTCATTGTCAT-3'. The housekeeping gene Gapdh was used as internal control. The qPCR procedure was repeated three times in independent runs; gene expression levels were calculated using the $\Delta\Delta C_T$ method.

**Protein extraction and western blotting**: Protein was extracted from the pressure-overloaded myocardium using T-Per Tissue Protein Extraction Reagent (Thermo Fisher Scientific, cat#78510) containing a cocktail of 10% protease and 10% phosphatase inhibitors (Thermo Fisher Scientific, cat#78429) as previously described [17]. Briefly, organs (heart and spleen) were removed, quickly frozen in liquid nitrogen and homogenized using a

tissue homogenizer. Protein lysates were spun at 10,000xg for 5 min at 4◦C, supernatant was collected and protein concentration was measured following a standard BCA method. An equal amount of proteins (30ug) under denaturing conditions was then subjected to SDS-PAGE (4-20%) followed by Western blotting analysis. Western blotting was performed using antibodies to p-Smad3 (Ser423/425, dilution 1:1000, Cell Signaling Technology, Danvers, MA), Smad3 (dilution 1:1000, Abcam, Cambridge, MA), Collagen type III (1:1000, Abcam, Cambridge, MA), p-p38 MAPK (1:1000, Cell Signaling Technology, #9215), p38 MAPK (1:1000, Cell Signaling Technology, #9212), pErk (1:1000, Cell Signaling Technology, #4376), Erk (1:1000, Cell Signaling Technology, #4695), pAkt (1:1000, Cell Signaling Technology, #4058), Akt (1:1000, Cell Signaling Technology, #9272), and GAPDH (dilution 1:1000, Santa Cruz Biotechnology, CA), as previously described [9], [14]. The gels were imaged by ChemiDoc™ MP System (Bio Rad) and analyzed by Image Lab 3.0 software (Bio Rad).

**Statistics**: Sample size estimates were based on our own experience with comparable experimental studies to achieve 90% power at a significance level of 0.05. For all analyses, normal distribution was tested using the Shapiro-Wilk normality test. For comparisons of two groups unpaired, 2-tailed Student's t-test using (when appropriate) Welch's correction for unequal variances was performed. The Mann-Whitney test was used for comparisons between 2 groups that did not show Gaussian distribution. For comparisons of multiple groups, 1-way ANOVA was performed followed by Tukey's multiple comparison test. The Kruskal-Wallis test, followed by Dunn's multiple comparison post-test was used when one or more groups did not show Gaussian distribution. Survival analysis was performed using the Kaplan-Meier method. Mortality was compared using the log rank test. The Fisher's exact test was used to compare replacement fibrosis. Data are expressed as means ± SEM. Statistical significance was set at 0.05.

## SUPPLEMENTAL FIGURES

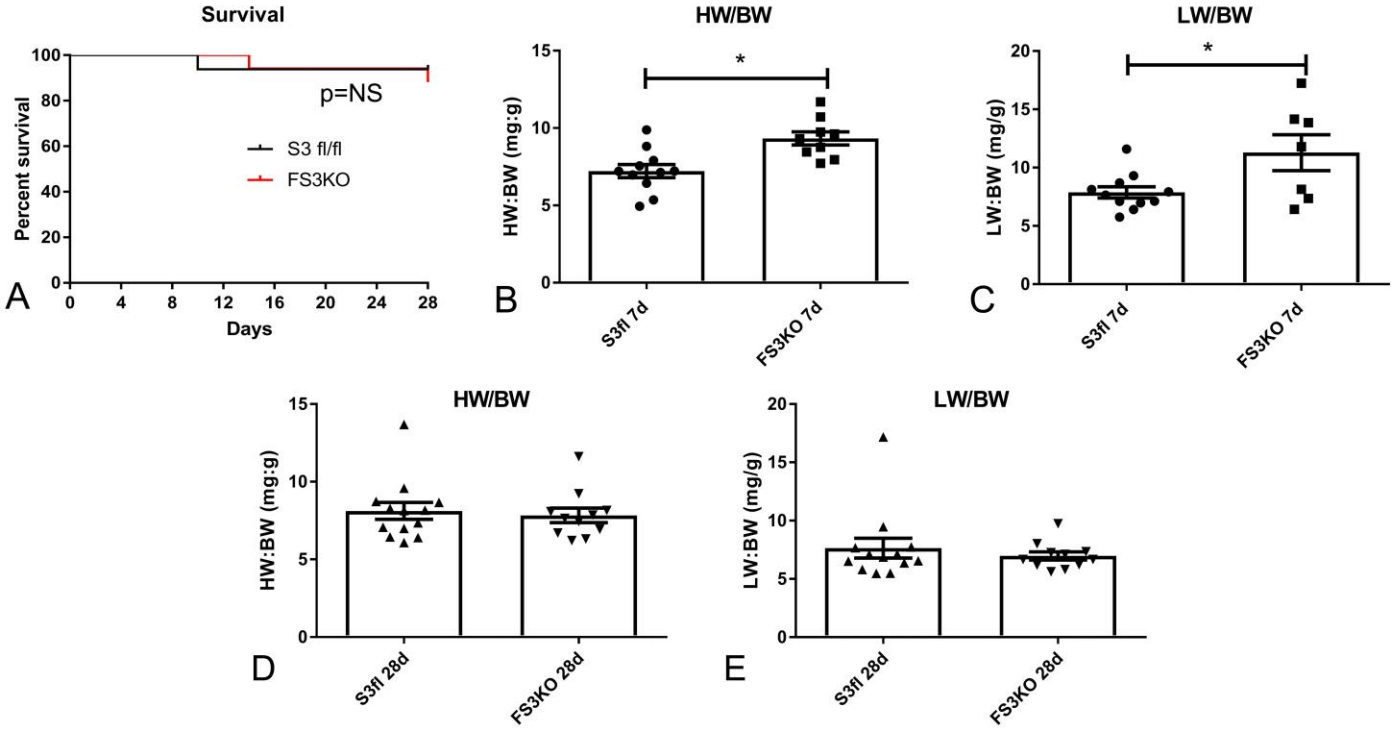


**Supplemental Figure I:** Effects of fibroblast-specific Smad3 loss on survival, heart weight and lung weight following pressure overload. A: Smad3 fl/fl and FS3KO mice exhibited comparable mortality following TAC (p=NS, n=30-33/group). B-C. After 7 days of TAC, FS3KO mice had significantly higher heart weight:body weight (HW:BW) ratio (*p<0.05) and lung weight:body weight (LW:BW) ratio than corresponding Smad3 fl/fl controls (*p<0.05). D-E: In contrast, no significant differences in HW:BW and LW:BW were noted after 28 days of TAC.

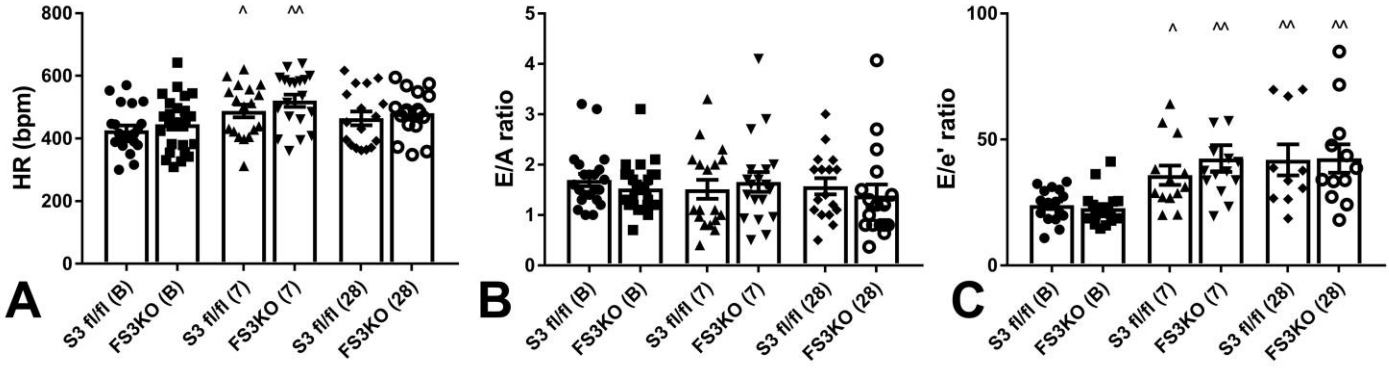


**Supplemental figure II**. Mitral inflow Doppler and tissue Doppler imaging were used to assess diastolic function. A: Both Smad3 fl/fl and FS3KO mice had increased HR after 7 days of TAC. B-C: Although no significant differences were noted in the E/A ratio, the E/e' ratio was markedly increased in both Smad3 fl/fl and FS3KO groups after 7-28 days of TAC. FS3KO and Smad3 fl/fl mice had comparable heart rate (A, HR), E:A ratio (B), and E/e' ratio (C) after 7 and 28 days of pressure overload, suggesting that fibroblast-specific Smad3 loss did not significantly affect diastolic function (^$p<0.05$, ^^$p<0.01$ vs. corresponding baseline values (B), n= 17-25/group).

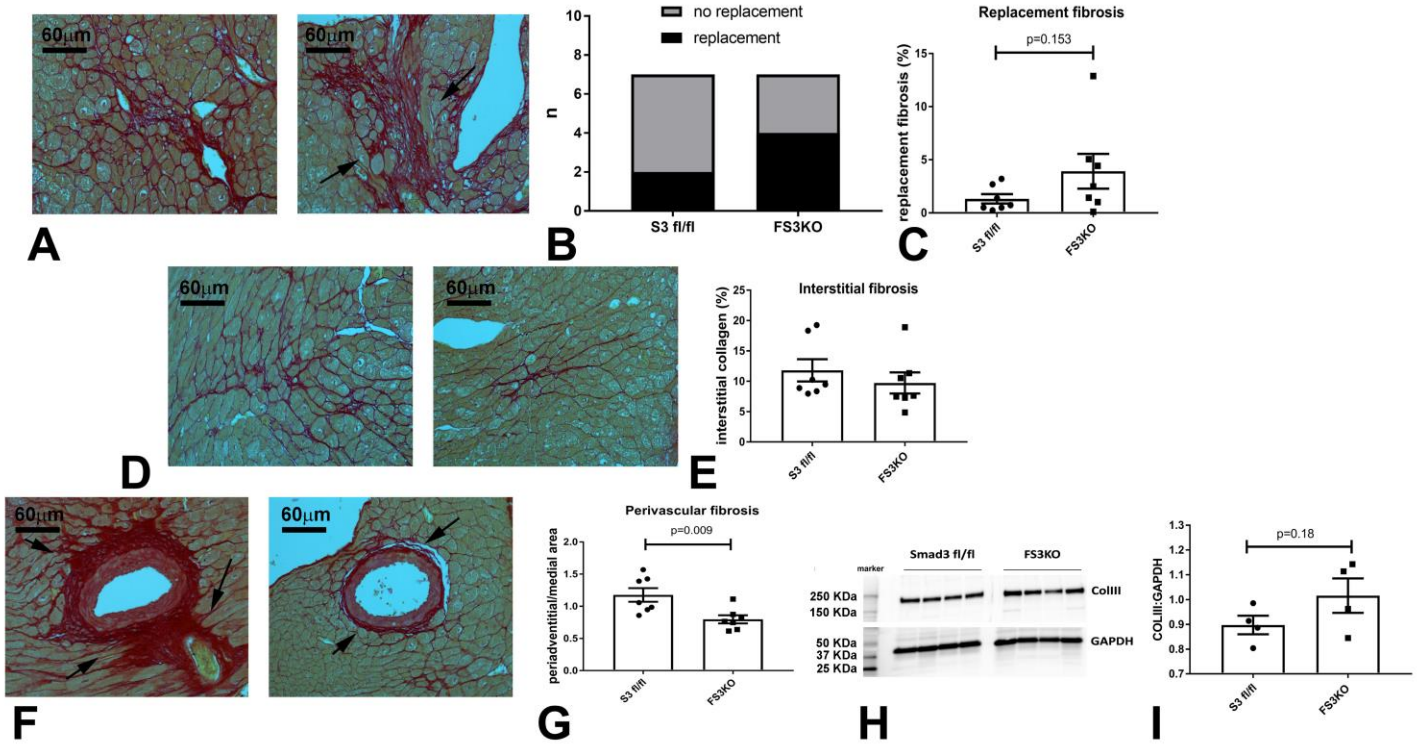


**Supplemental figure III**: Effects of fibroblast-specific Smad3 loss on cardiac fibrosis after 28 days of TAC. A-C: Foci of replacement fibrosis were identified as areas of cardiomyocyte replacement with collagen-based scar (arrows). FS3KO mice exhibited a trend towards increased replacement fibrosis (p=0.15, n=7/group). D-E. There was no significant difference in interstitial fibrosis between Smad3 fl/fl and FS3KO mice. F-G: FS3KO mice exhibited a reduction in perivascular fibrosis (arrows) evidenced by a lower periadventitial collagen:medial area (p=0.009). H-I: Western blotting with an antibody to collagen III showed no significant effects of fibroblast-specific Smad3 loss on collagen III levels (p=0.18, n=4/group). Collagen III, one of the classical fibrillar collagens, is a major component of myocardial collagen fibers.

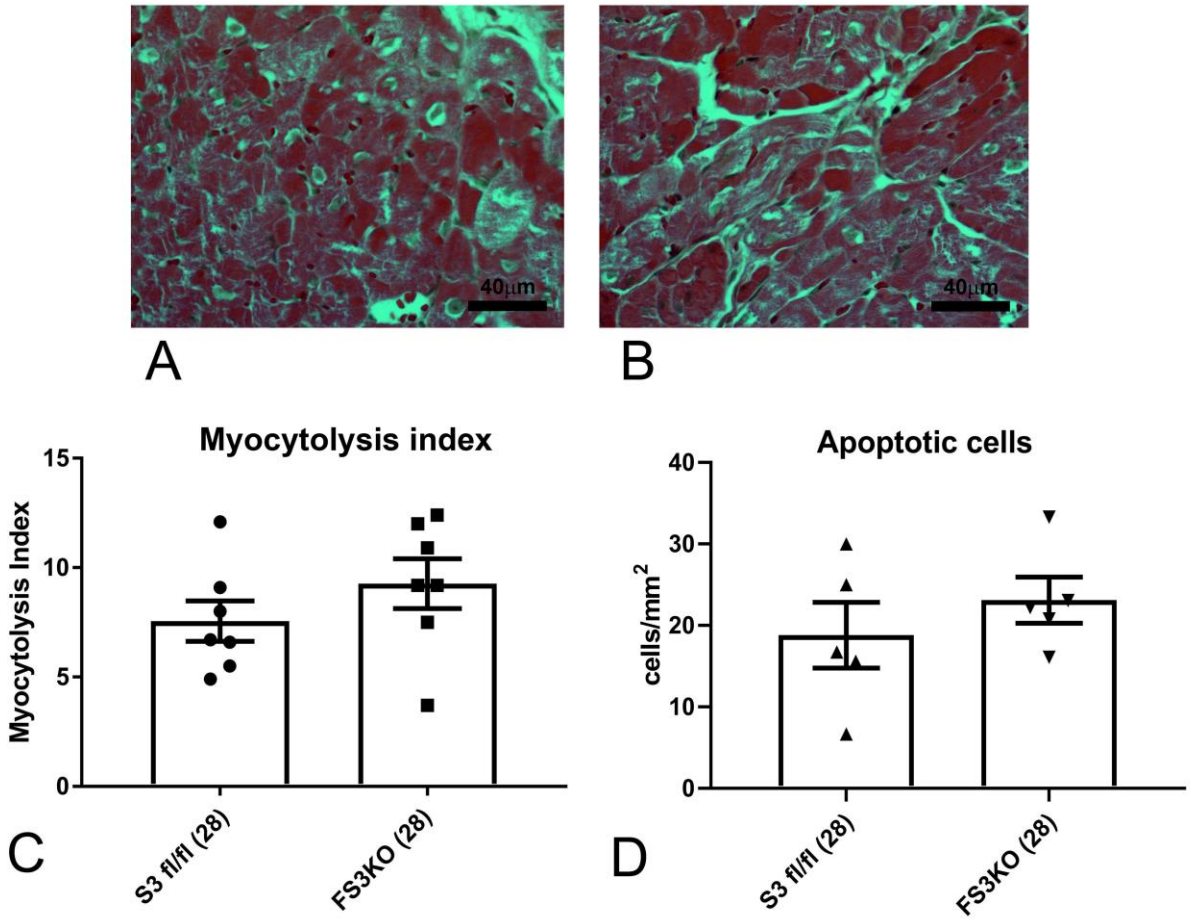


**Supplemental figure IV**: Effects of fibroblast-specific Smad3 loss on cardiomyocyte apoptosis after 28 days of TAC. A-C: Hematoxylin-eosin staining was used to assess degenerative changes in cardiomyocytes of the pressure-overloaded heart. Quantitative analysis of the myocytolysis index showed no significant differences between Smad3 fl/fl and FS3KO mice after 28 days of pressure overload. D: TUNEL staining showed that the density of apoptotic cells was not significantly different between groups after 28 days of TAC (p=NS, n=5-7/group).

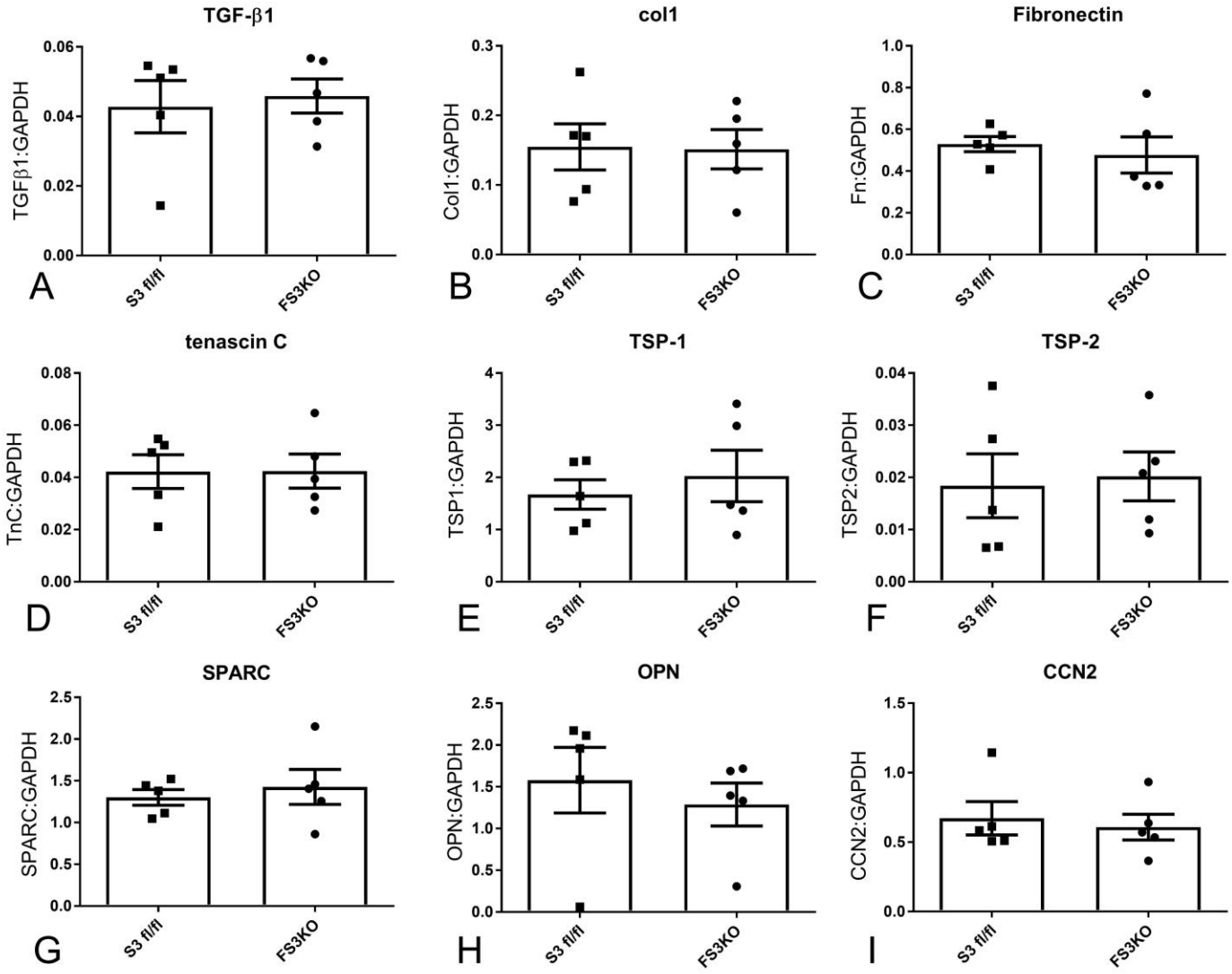


**Supplemental figure V**: Effects of fibroblast-specific Smad3 loss on expression of structural and matricelllular matrix proteins. Fibroblasts were harvested from Smad3 fl/fl and FS3KO hearts after 7 days of TAC. FS3KO and Smad3 fl/fl fibroblasts had no significant differences in expression of TGF-β1, collagen I, fibronectin and in synthesis of the matricellular proteins tenascin-C, thrombospondin -1 and 2 (TSP1, TSP2), SPARC, osteopontin (OPN) and CCN2 (p=NS, n=5/group).

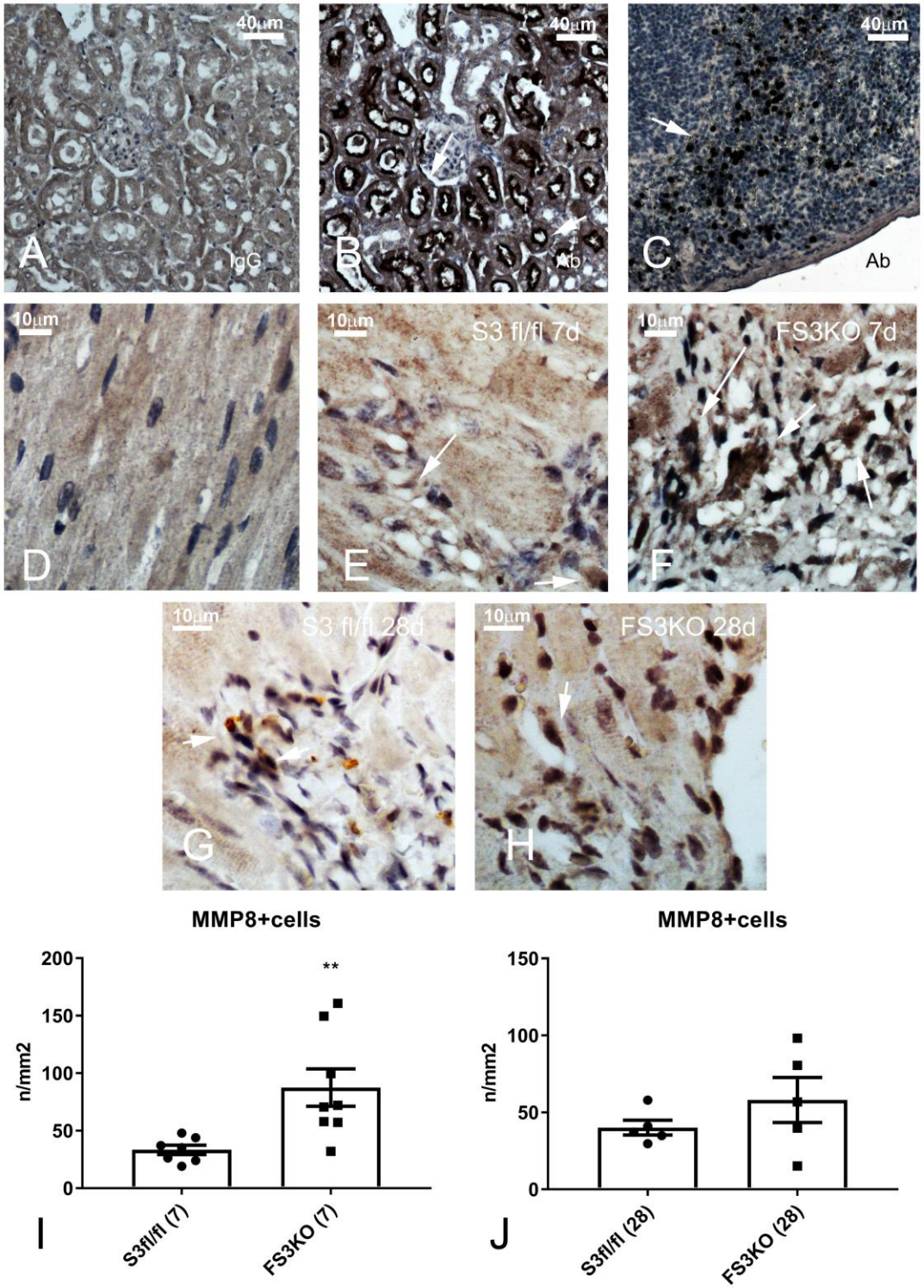


**Supplemental figure VI**: Fibroblast-specific Smad3 loss is associated with increased MMP8 expression in the cardiac interstitium. A-C: Validation of the anti-MMP8 antibody. Immunohistochemical staining with isotype matched IgG showed no significant staining in mouse kidney (A), whereas staining with the anti-MMP8 antibody shows labeling of renal tubules (B) and of splenic cells (C). Immunohistochemical staining of normal (D) and pressure-overloaded myocardium after 7 (E-F) and 28 days (G-H) showed increased infiltration of the cardiac interstitium with MMP8+ cells in FS3KO mice after 7 days of TAC (arrows). Quantitative analysis

demonstrated a markedly increased number of MMP8+ interstitial cells in FS3KO mice after 7 days of TAC (**$p<0.01$, n=7-8/group). However, after 28 days of pressure overload, there was no significant difference in the density of MMP8+ cells between groups.

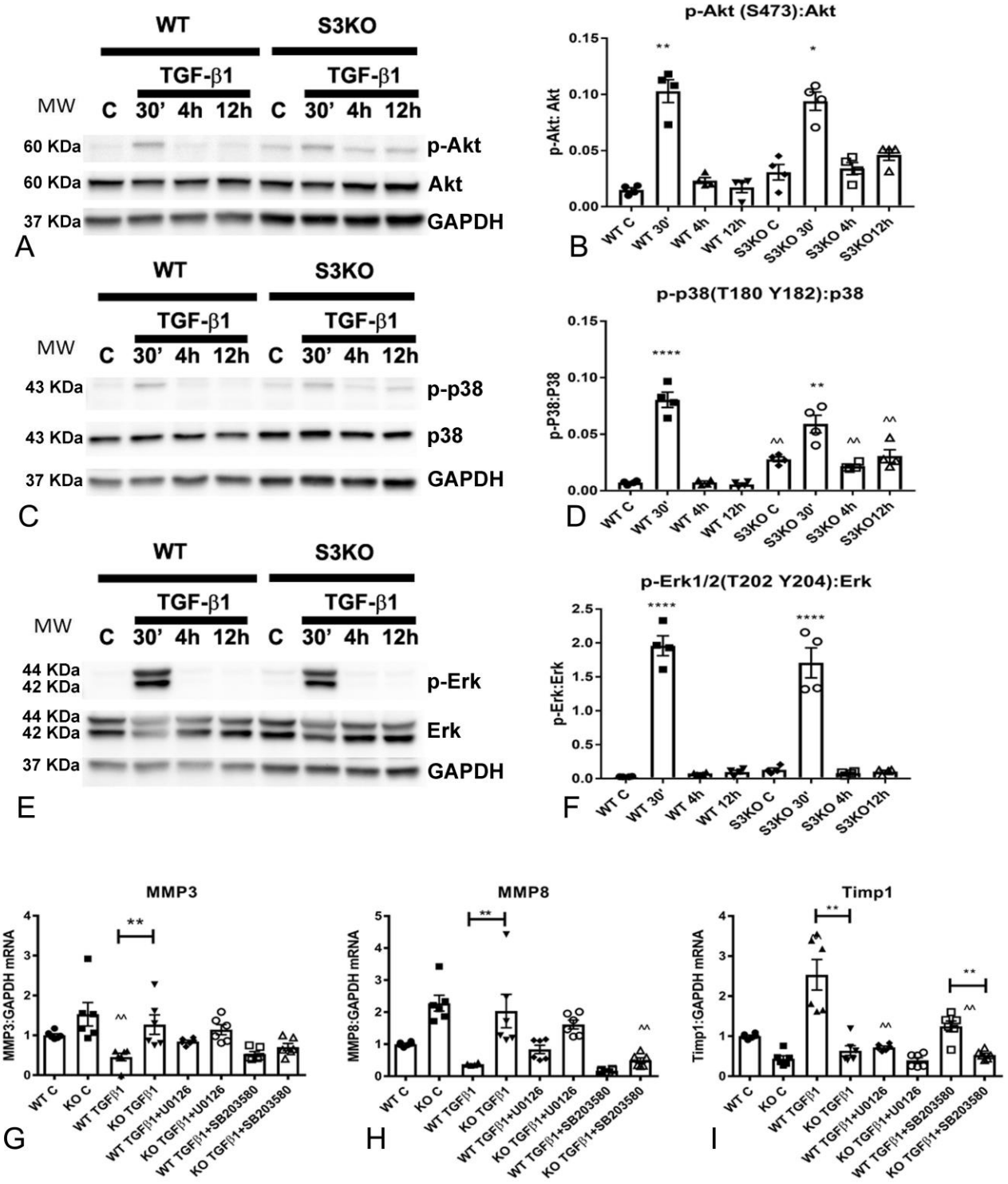


**Supplemental figure VII**: Role of non-Smad pathways in mediating the matrix-preserving actions of TGF-β1 in cardiac fibroblasts. A-F: Western blotting experiments show that TGF-β1 rapidly activates Akt, p38 MAPK, and Erk MAPK signaling in both WT and Smad3 KO (S3KO) cardiac fibroblasts (cells harvested from mice with global loss of Smad3). A-B: After 30 min of stimulation, TGF-β1 (10ng/ml) significantly increased the p-Akt:Akt expression ratio in both WT and Smad3 KO cells. C-D: TGF-β1 also increased the p-p38: p38 MAPK ratio in both WT and Smad3 KO cells. Smad3 KO cells had a modest, but significant increase in p-p38 MAPK

activation at baseline and after 4-12 h of stimulation, but not at the timepoint of peak activation (30 min). E-F: TGF-β1 also increased the pErk:Erk ratio in both WT and Smad3 KO cells. These findings document Smad3-independent activation of Akt, p38 MAPK and Erk MAPK in cardiac fibroblasts (*p<0.05, **p<0.01, ****p<0.0001 vs. corresponding unstimulated cells; ^^p<0.01 vs. corresponding WT cells, n=4). G-I: The role of Smad-independent pathways on the effects of TGF-β1 in regulation of MMP and TIMP synthesis in cardiac fibroblasts cultured in collagen pads. mRNA levels of MMP3 (G), MMP8 (H) and TIMP1 (I) were assessed after 24h of stimulation. Levels were normalized to WT control cells. Smad3 KO cells had higher baseline levels of MMP8 (H, **p<0.01 vs. WT control). TGF-β1 stimulation suppressed MMP3 (G) and MMP8 (H) mRNA synthesis (^^p<0.01 vs. control) in WT cells but not in Smad3 KO cells. In WT cells, Erk inhibition with U0126, but not p38 MAPK inhibition with SB203580 abrogated the suppressive effects of TGF-β1 on MMP3 and MMP8 synthesis (##p<0.01 vs. WT TGF-β). In contrast, in Smad3 KO cells, Erk inhibition did not affect MMP3 and MMP8 synthesis suggesting that the effects of Erk in mediating the suppressive effects of TGF–β1 are not independent of Smad3. (@@p<0.01 vs. KO TGF-β). I: TGF-β1 induced TIMP1 in WT cells, but not in Smad3 KO cells (^^p<0.01 vs. WT control). In WT cells, both Erk and p38 MAPK inhibition attenuated TGF-β1-induced TIMP-1 synthesis (##p<0.01 vs. WT TGF-β). In contrast, in Smad3 KO cells neither the Erk inhibitor, not the p38 MAPK inhibitor had any effects on TIMP-1 levels, suggesting that the effects of Erk and p38 MAPK on TIMP-1 expression were Smad3-dependent (n=6).

REFERENCES:


1. Lindsley A, Snider P, Zhou H, Rogers R, Wang J, Olaopa M, Kruzynska-Frejtag A, Koushik SV, Lilly B, Burch JB, Firulli AB and Conway SJ. Identification and characterization of a novel Schwann and outflow tract endocardial cushion lineage-restricted periostin enhancer. *Dev Biol*. 2007;307:340-55.
2. Takeda N, Manabe I, Uchino Y, Eguchi K, Matsumoto S, Nishimura S, Shindo T, Sano M, Otsu K, Snider P, Conway SJ and Nagai R. Cardiac fibroblasts are essential for the adaptive response of the murine heart to pressure overload. *J Clin Invest*. 2010;120:254-65.
3. Conway SJ and Molkentin JD. Periostin as a heterofunctional regulator of cardiac development and disease. *Curr Genomics*. 2008;9:548-55.
4. Kong P, Christia P, Saxena A, Su Y and Frangogiannis NG. Lack of specificity of fibroblast-specific protein 1 in cardiac remodeling and fibrosis. *Am J Physiol Heart Circ Physiol*. 2013;305:H1363-72.
5. Oka T, Xu J, Kaiser RA, Melendez J, Hambleton M, Sargent MA, Lorts A, Brunskill EW, Dorn GW, 2nd, Conway SJ, Aronow BJ, Robbins J and Molkentin JD. Genetic manipulation of periostin expression reveals a role in cardiac hypertrophy and ventricular remodeling. *Circ Res*. 2007;101:313-21.
6. Li Q, Pangas SA, Jorgez CJ, Graff JM, Weinstein M and Matzuk MM. Redundant roles of SMAD2 and SMAD3 in ovarian granulosa cells in vivo. *Mol Cell Biol*. 2008;28:7001-11.
7. Kong P, Shinde A, Su Y, Russo I, Chen B, Saxena A, Conway SJ, Graff JM and Frangogiannis NG. Opposing actions of fibroblast and cardiomyocyte Smad3 signaling in the infarcted myocardium. *Circulation*. 2017 (in press).
8. Xia Y, Lee K, Li N, Corbett D, Mendoza L and Frangogiannis NG. Characterization of the inflammatory and fibrotic response in a mouse model of cardiac pressure overload. *Histochem Cell Biol*. 2009;131:471-81.
9. Xia Y, Dobaczewski M, Gonzalez-Quesada C, Chen W, Biernacka A, Li N, Lee DW and Frangogiannis NG. Endogenous thrombospondin 1 protects the pressure-overloaded myocardium by modulating fibroblast phenotype and matrix metabolism. *Hypertension*. 2011;58:902-11.
10. Dobaczewski M, Xia Y, Bujak M, Gonzalez-Quesada C and Frangogiannis NG. CCR5 signaling suppresses inflammation and reduces adverse remodeling of the infarcted heart, mediating recruitment of regulatory T cells. *Am J Pathol*. 2010;176:2177-87.
11. Dobaczewski M, Bujak M, Li N, Gonzalez-Quesada C, Mendoza LH, Wang XF and Frangogiannis NG. Smad3 signaling critically regulates fibroblast phenotype and function in healing myocardial infarction. *Circ Res*. 2010;107:418-28.
12. Zitnay JL, Li Y, Qin Z, San BH, Depalle B, Reese SP, Buehler MJ, Yu SM and Weiss JA. Molecular level detection and localization of mechanical damage in collagen enabled by collagen hybridizing peptides. *Nature communications*. 2017;8:14913.
13. Hwang J, Huang Y, Burwell TJ, Peterson NC, Connor J, Weiss SJ, Yu SM and Li Y. In Situ Imaging of Tissue Remodeling with Collagen Hybridizing Peptides. *ACS Nano*. 2017;11:9825-9835.
14. Rowe SM, Jackson PL, Liu G, Hardison M, Livraghi A, Solomon GM, McQuaid DB, Noerager BD, Gaggar A, Clancy JP, O'Neal W, Sorscher EJ, Abraham E and Blalock JE. Potential role of high-mobility group box 1 in cystic fibrosis airway disease. *Am J Respir Crit Care Med*. 2008;178:822-31.
15. Shinde AV, Humeres C and Frangogiannis NG. The role of alpha-smooth muscle actin in fibroblast-mediated matrix contraction and remodeling. *Biochim Biophys Acta*. 2017;1863:298-309.
16. Stanley ER. Murine bone marrow-derived macrophages. *Methods Mol Biol*. 1997;75:301-4.
17. Shinde AV, Su Y, Palanski BA, Fujikura K, Garcia MJ and Frangogiannis NG. Pharmacologic inhibition of the enzymatic effects of tissue transglutaminase reduces cardiac fibrosis and attenuates cardiomyocyte hypertrophy following pressure overload. *J Mol Cell Cardiol*. 2018;117:36-48.